

# A GFP-based assay reveals a role for RHD3 in transport between the endoplasmic reticulum and Golgi apparatus

Huanquan Zheng<sup>1,2,i</sup>, Ljerka Kunst<sup>3</sup>, Chris Hawes<sup>2</sup> and Ian Moore<sup>1,\*</sup>

<sup>1</sup>Department of Plant Sciences, University of Oxford, South Parks Road, Oxford OX1 3RB, UK,

<sup>2</sup>Research School of Biological & Molecular Sciences, Oxford Brookes University, Gypsy Lane, Oxford OX3 0BP, UK, and

<sup>3</sup>Department of Botany, University of British Columbia, 3529-6270 University Boulevard, Vancouver, BC, Canada V6T 1Z4

Received 12 August 2003; revised 21 October 2003; accepted 28 October 2003.

\*For correspondence (fax +44 1865 275074; e-mail ian.moore@plants.ox.ac.uk).

<sup>i</sup>Present address: Department of Botany, University of British Columbia, 3529-6270 University Boulevard, Vancouver, BC, Canada V6T 1Z4.

---

## Summary

We describe the use of a secreted form of *Aequoria victoria* green fluorescent protein (secGFP) in a non-invasive live cell assay of membrane traffic in *Arabidopsis thaliana*. We show that in comparison to GFP-HDEL, which accumulates in the endoplasmic reticulum (ER), secGFP generates a weak fluorescence signal when transported to the apoplast. The fluorescence of secGFP in the apoplast can be increased by growth of seedlings on culture medium buffered at pH 8.1, suggesting that apoplastic pH is responsible, at least in part, for the low fluorescence intensity of seedlings expressing secGFP. Inhibition of secGFP transport between the ER and plasma membrane (PM), either by Brefeldin A (BFA) treatment or by genetic intervention results in increased intracellular secGFP accumulation accompanied by an increase in the secGFP fluorescence intensity. secGFP thus provides a valuable tool for forward and reverse genetic analysis of membrane traffic and endomembrane organisation in *Arabidopsis*. Using this assay for quantitative sub-lethal perturbation of secGFP transport, we identify a role for root hair defective 3 (RHD3) in transport of secreted and Golgi markers between the ER and the Golgi apparatus.

**Keywords:** GFP, endoplasmic reticulum, Golgi, membrane traffic, root hair defective 3.

---

## Introduction

Plant cells, like other eukaryotic cells, are characterised by an elaborate endomembrane system that includes the endoplasmic reticulum (ER), Golgi apparatus, vacuole and plasma membrane (PM). Membrane traffic between organelles of the endomembrane system is essential for plant cell division, growth, differentiation and function during development. Detailed molecular and genetic analyses in the unicellular budding yeast *Saccharomyces cerevisiae* and many specialised mammalian cells revealed that cells have evolved complex regulatory mechanisms to ensure accurate and efficient membrane trafficking between specific compartments of the endomembrane system. These mechanisms involve a multitude of proteins, either specific for a particular trafficking event or general for multiple transport stages (Mellman and Warren, 2000). The *Arabidopsis* genome project has revealed the existence of many homologues of yeast genes involved in membrane traffic, but only recently, some of them have been confirmed to play a role in specific membrane

trafficking events (Assaad *et al.*, 2001; Batoko *et al.*, 2000; Cheung *et al.*, 2002; Geelen *et al.*, 2002; Geldner *et al.*, 2003; Kim *et al.*, 2001; Pimpl *et al.*, 2003; Sohn *et al.*, 2003; Steinmann *et al.*, 1999; Takeuchi *et al.*, 2000, 2002). One of the major obstacles in studying membrane traffic in plants is the lack of convenient markers that can be used to report traffic events.

Many of the recent studies of membrane trafficking mechanisms have utilised the jellyfish green fluorescent protein (GFP) as a visual marker of protein trafficking in various transient expression systems (Batoko *et al.*, 2000; Boevink *et al.*, 1999; Cheung *et al.*, 2002; Geelen *et al.*, 2002; Kim *et al.*, 2001; Sohn *et al.*, 2003; Takeuchi *et al.*, 2000, 2002). For example, by transient co-expression of dominant inhibitory Rab GTPase mutants with a secreted form of *Aequoria victoria* green fluorescent protein (secGFP) – a GFP fusion that is transported from the ER to the extracellular space (Batoko *et al.*, 2000) – we reported that a Rab1 protein was required for ER-to-Golgi traffic (Batoko *et al.*,

2000) and that the soluble *N*-ethylmaleimide sensitive factor attachment protein receptor (SNARE) protein Nt-Syr1 (NtSyp121) was probably involved in post-Golgi membrane traffic (Geelen *et al.*, 2002). Many key protein families controlling endomembrane traffic can be predicted from their similarity to known yeast proteins and some can be readily modified to generate dominant inhibitory forms. These include some of the most important families such as the Rab GTPases and SNAREs. In *Arabidopsis*, these protein families are several times greater than those in yeast and are different in composition to those of mammals (Rutherford and Moore, 2002; Sanderfoot *et al.*, 2000). The differences in Rab GTPase and SNARE complement most probably reflect differences in membrane trafficking events that occur in each group of organisms. Transient expression systems provide a means to test the functions of these conserved protein families in amenable cell types. However, the approach has clear limitations. The interpretation of phenotypes generated by dominant negative mutants is not simple, and not all proteins can be readily converted to dominant inhibitory forms.

The plant endomembrane system is morphologically distinct from the mammalian system and interacts differently with the cytoskeleton (Boevink *et al.*, 1998; Brandizzi *et al.*, 2002; Nebenführ *et al.*, 1999), so it may not be possible to identify the underlying molecular machinery by similarity to yeast and mammalian sequences. Multicellularity arose independently in the animal and plant lineages, so it is likely that higher plants, like mammals, have evolved tissue-specific membrane traffic pathways or specific modifications of the common regulatory machinery to facilitate some of the characteristic aspects of plant development and cell function. Known examples include cell plate formation, polarised distribution of membrane proteins and protein sorting to distinct vacuoles (Jurgens and Geldner, 2002). Molecular components of each of these processes have been identified by genetic and biochemical means (Ahmed *et al.*, 2000; Lukowitz *et al.*, 1996; Steinmann *et al.*, 1999). It is also noteworthy that extreme environmental conditions (Bolte *et al.*, 2000), as well as pathogen attack (Bogdanove and Martin, 2000), evoke expression of Rab GTPases. It is not clear that these processes can be studied in cell types, such as protoplasts and leaf epidermal cells, which are most amenable to transient expression.

In yeast, the combination of genetic and biochemical assays has led to the isolation of secretory mutants that have allowed an incisive analysis of many important steps in the secretory pathway (Mellman and Warren, 2000). In *Arabidopsis*, the mutagenesis approach is standard for the genetic dissection of many developmental and biochemical processes. Some mutants such as *gnom*, *knolle*, *keule* and *vac1*, which were initially identified by virtue of their defect in embryo development, have subsequently been

found to encode components of the plant membrane trafficking pathways (Assaad *et al.*, 2001; Lukowitz *et al.*, 1996; Rojo *et al.*, 2001; Shevell *et al.*, 1994). However, the lack of predictable phenotypes and convenient assays has hindered the systematic isolation of mutants defective in various membrane-transport processes. To facilitate systematic studies of gene function in membrane traffic during plant development, we developed a visual screen and biochemical assay system for potential mutants with perturbed endomembrane dynamics. The principle of the assay is similar to the transient expression assay using secGFP reported previously for tobacco epidermal cells (Batoko *et al.*, 2000). It exploits the observation that GFP exhibits strong fluorescence when it accumulates in the ER or Golgi, but fails to accumulate in a fluorescent form if it is transported to the apoplast. Furthermore, transport of secGFP from the ER to the apoplast is accompanied by a carboxyl-terminal proteolytic event that is readily detected by gel electrophoresis. To demonstrate the utility of the secGFP assay, we have used the system to investigate ER-to-Golgi transport in root hair defective 3 (*rhd3*) mutant.

*rhd3* was originally isolated because it exhibits short roots and short wavy root hairs in comparison to wild-type (wt) roots (Schiefelbein and Somerville, 1990). *RHD3* encodes an 89-kDa protein with putative GTP-binding motifs near the amino-terminal region (Wang *et al.*, 1997). Detailed study of the expression and regulation of *RHD3* gene found that it is expressed in all major *Arabidopsis* organs, and multiple levels of regulation are employed to ensure appropriate expression of the gene (Wang *et al.*, 2002), indicating that *RHD3* is not root-hair-specific. The major defect in *rhd3* mutants is reduced cell size, particularly in longitudinal axis, and it has been interpreted to have defects in the orientation and extent of cell expansion, but not in cell number (Wang *et al.*, 1997). Galway *et al.* (1997) reported that the *rhd3* mutant has a reduced vacuole and an abnormally large quantity of vesicles in the subapical region of root hairs, whereas vesicles are primarily located in the apical regions of wt root hairs. These observations led to the hypothesis that the phenotype of *rhd3* mutant cells might result from impaired vacuole biogenesis or from uneven or reduced deposition of secretory vesicles during cell elongation. However, there has been no direct test to establish whether *RHD3* indeed plays a role in endomembrane traffic from the ER to the PM in expanding cells.

Using the secGFP assay, we present evidence that *RHD3* is required for normal rates of membrane traffic between the ER and Golgi and for normal ER organisation. The data indicate that secGFP, when expressed in *Arabidopsis*, can be used for the direct analysis of mutants and identification of genes involved in endomembrane dynamics in the secretory pathway.

## Results

### *Transgenic Arabidopsis reveals differential fluorescence between secGFP and GFP-HDEL lines*

To develop an *in vivo* visual screen and assay system for the analysis of membrane traffic in *Arabidopsis*, we used plasmids pVKH18-secGFP and pVKH18-GFP-HDEL described by Batoko *et al.* (2000). These plasmids direct expression of secGFP and GFP-HDEL respectively. We previously showed that when transiently expressed in tobacco leaf epidermis, secGFP was transported to the apoplast and exhibited weak fluorescence in comparison to GFP-HDEL, which accumulated in the ER by virtue of its carboxyl-terminal His-Asp-Glu-Leu (HDEL) retrieval signal (Batoko *et al.*, 2000). *Arabidopsis* was transformed with each plasmid and GFP fluorescence intensity was examined in T<sub>2</sub> seedlings of 9 independent GFP-HDEL and 20 independent secGFP transformants that were phenotypically normal and inherited the T-DNA as a single Mendelian locus (Chi-square data not shown). In each population, a range of fluorescence intensities was observed (Figure 1), but the secGFP lines (Figure 1g,i,k) generally exhibited weaker fluorescence than the GFP-HDEL lines (Figure 1a,c,e) in all tissues and at all developmental stages. Fluorescence intensity in the brightest secGFP line, S76 (Figure 1g), was lower than in most of the GFP-HDEL lines. Fluorescence

intensity in roots was stronger than in shoots, probably reflecting the properties of the 35S promoter used (Jefferson *et al.*, 1987). Lines S76 and H13 exhibited the strongest secGFP and GFP-HDEL fluorescence, respectively, and were chosen for further study.

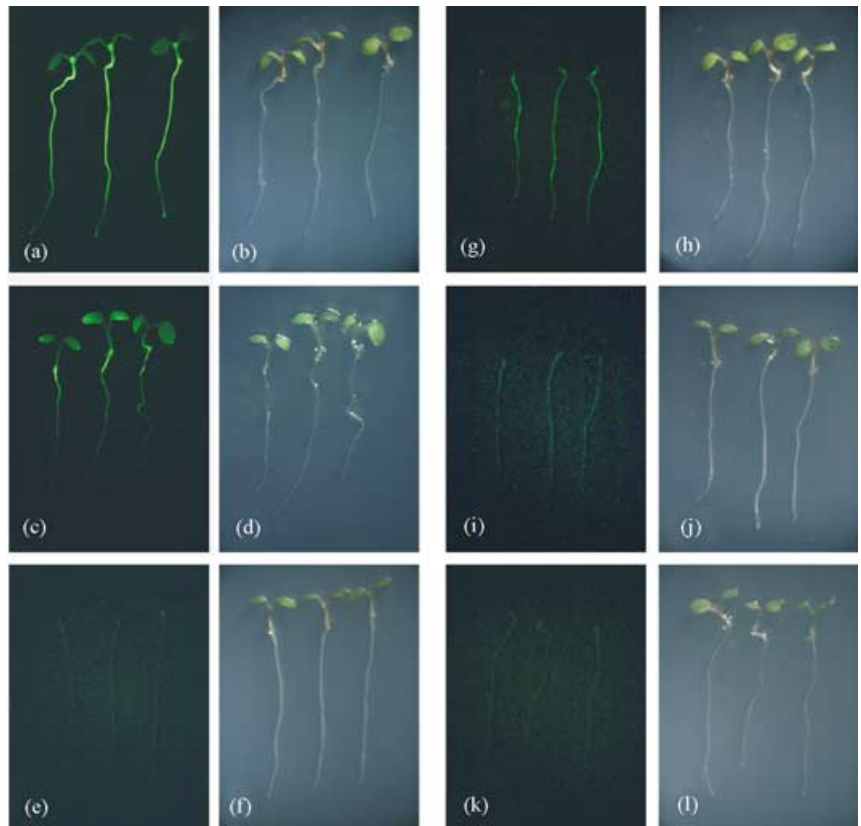
Higher magnification examination of the GFP-HDEL line H13 by confocal microscopy revealed GFP fluorescence in a typical ER network and fusiform bodies with bright fluorescence (Haseloff *et al.*, 1997; Figure 2a). Recent evidence has suggested that these fusiform bodies, labelled by GFP-HDEL, reside within the ER lumen (Hawes *et al.*, 2001) and were induced under stress conditions (Matsushima *et al.*, 2003). In comparison to H13, GFP fluorescence from the secGFP line S76 was much dimmer. When S76 was examined with the same imaging conditions used for H13, some fusiform bodies with weak fluorescence were detectable in mature root epidermal cells (Figure 2b), but the ER network was not detectable. No GFP fluorescence was seen in the apoplast either. When more sensitive imaging parameters were used, fluorescence was detectable in the ER network, but we were still unable to detect it in the apoplast.

### *secGFP accumulates less efficiently than GFP-HDEL in seedlings*

In tobacco, differential fluorescence between secGFP and GFP-HDEL is, at least in part, because of reduced GFP

**Figure 1.** Comparison of GFP fluorescence between secGFP and GFP-HDEL-expressing *Arabidopsis* lines.

(a–f) Fluorescent (a,c,e) and bright-field (b,d,f) images of seedlings of the transgenic GFP-HDEL lines H13 (a,b), H27 (c,d) and H16 (e,f) emitting different levels of GFP fluorescence. (g–l) Fluorescent (g,i,k) and bright-field (h,j,l) images of seedlings of the transgenic secGFP lines S76 (g,h), S8 (i,j) and S18 (k,l) showing different levels of GFP fluorescence.



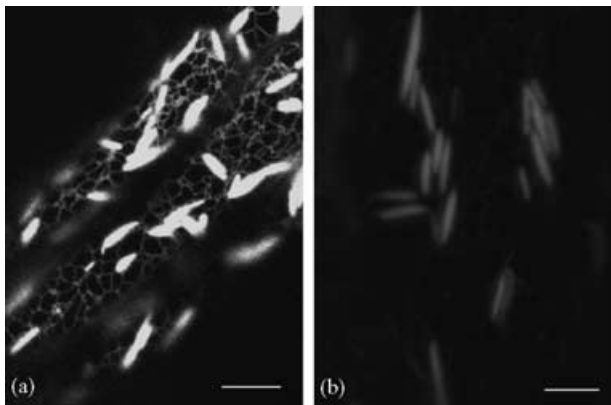


**Figure 2.** The localisation of GFP fluorescence in transgenic *Arabidopsis* expressing either GFP-HDEL or secGFP.

(a) Confocal laser scanning microscopy image of the transgenic H13 line expressing GFP-HDEL in mature root cells showing the commonly described open ER polygonal network and the fusiform bodies. Bar = 10 µm.

(b) Confocal micrograph of GFP fluorescence in mature cells of a root of the S76 line expressing secGFP showing some fusiform bodies. Bar = 10 µm.

accumulation in secGFP-expressing tissues. secGFP was transported to the apoplast via a Brefeldin A (BFA)-sensitive pathway, and during this transport, GFP was subjected to proteolysis (Batoko *et al.*, 2000). We therefore investigated whether similar mechanisms operated in *Arabidopsis*.

Total proteins were extracted from roots of three GFP-HDEL lines and three secGFP lines that represented the range of fluorescence exhibited by each transgenic population. Protein probed with anti-GFP revealed that both secGFP and GFP-HDEL accumulation correlated positively with the intensity of GFP fluorescence exhibited in the respective population (Figure 3a). GFP accumulation in the population of secGFP lines was, however, generally lower than in the GFP-HDEL lines (S76 versus H13, S8 versus H27 and S18 versus H16; Figure 3a). This indicated that the lower fluorescence of the secGFP lines was, at least in part, related to lower secGFP accumulation.

To establish whether the reduced accumulation of secGFP arose from reduced steady-state mRNA abundance, we analysed secGFP and GFP-HDEL transcript levels in the lines investigated by Western blot. We found that secGFP transcripts were not less abundant than GFP-HDEL transcripts (Figure 3b). In secGFP line S76, which exhibited the highest GFP fluorescence intensity of over 100 pVKH18-secGFP primary transformants, the secGFP mRNA level (Figure 3b, lane S76) was comparable to that of GFP-HDEL line H13 (Figure 3b, lane H13), which exhibited substantially higher fluorescence and GFP accumulation. This indicated that low GFP protein accumulation in secGFP lines, relative to GFP-HDEL lines, cannot be explained by secGFP mRNA abundance. This result is consistent with other studies of artificial secretory proteins (Denecke *et al.*, 1990; Wandelt *et al.*, 1992).

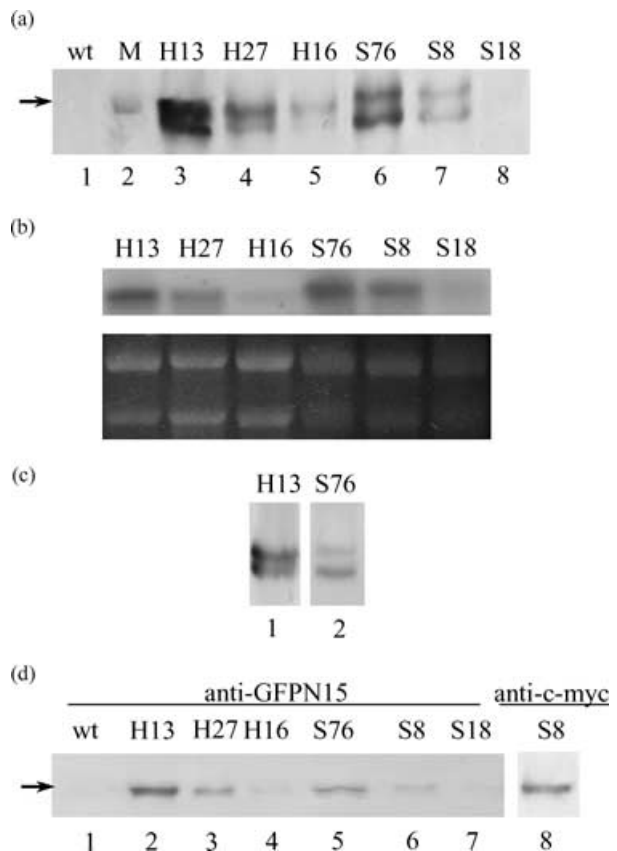


**Figure 3.** secGFP accumulates less efficiently than GFP-HDEL in seedlings, although both are subjected to a C-terminal proteolysis.

(a) Immunoblot analysis of protein extracts from roots of transgenic GFP-HDEL lines H13 (lane 3), H27 (lane 4) and H16 (lane 5) and secGFP lines S76 (lane 6), S8 (lane 7) and S18 (lane 8). The immunodetection was carried out with an antiserum against full-length GFP (anti-GFP). Lane 1 shows wt *Arabidopsis* and lane 2 contains molecular weight markers. The arrow indicates a molecular weight of 30 kDa.

(b) RNA blot analysis of total RNAs extracted from roots of transgenic *Arabidopsis* lines S76, S8 and S18 that express secGFP, and lines H13, H27 and H16 that express GFP-HDEL.

(c) Immunoblot analysis of shoots of transgenic GFP-HDEL line H13 (lane 1) and secGFP line S76 (lane 2) revealed the same GFP-accumulation pattern as that in roots (a).

(d) Immunoblot analysis of the same protein extracts as in (a) with anti-GFPN15 (antiserum against C-terminal peptides of GFP; lanes 1–7) and anti-c-myc for secGFP line S8 (lane 8) indicating that the lower GFP band is C-terminally truncated. The arrow indicates molecular weight of 30 kDa.

#### *secGFP and GFP-HDEL are subjected to C-terminal proteolysis to different extents*

In roots, GFP-HDEL predominantly accumulated as a band, which migrated with an apparent molecular weight of slightly less than 30 kDa (Figure 3a, lanes 3–5). The band was associated with a less intense band that was approximately 2 kDa smaller than expected. Two similar bands were detected when shoot tissues of line H13 were examined (Figure 3c, lane 1). secGFP also exhibited two bands in root (Figure 3a, lanes 6–8), as well as shoot extracts, as

exemplified by S76 (Figure 3c, lane 2). The upper band appeared to migrate at the expected position for full-length secGFP with an apparent molecular weight approximately 1 kDa greater than that of the predominant GFP-HDEL band, owing to the *c-myc* epitope tag at its carboxyl terminus (Batoko *et al.*, 2000). The lower secGFP band migrated to the same position as the minor GFP-HDEL species. However, in contrast to the GFP-HDEL lines, this lower band was either the predominant secGFP band (line S76; Figure 3a, lane 6) or was of similar intensity to the upper band (line S8; Figure 3a, lane 7). To investigate the nature of the lower molecular weight secGFP and GFP-HDEL bands, proteins were probed with anti-GFPN15, an antibody raised against a carboxyl-terminal peptide of GFP, and with anti-*c-myc*. Both anti-GFPN15 and anti-*c-myc* recognised the upper secGFP band, but failed to recognise the lower band (Figure 3d, lanes 5–8), indicating that the predominant secGFP species had been truncated at its carboxyl terminus. Anti-GFPN15 also failed to bind the lower GFP-HDEL band (Figure 3d, lanes 2–4), suggesting that the small portion of GFP-HDEL had undergone a similar carboxyl-terminal truncation.

#### *secGFP is present in the apoplast in a truncated form*

As we were unable to detect apoplastic GFP fluorescence even in line S76, protoplast and apoplast fractions of lines

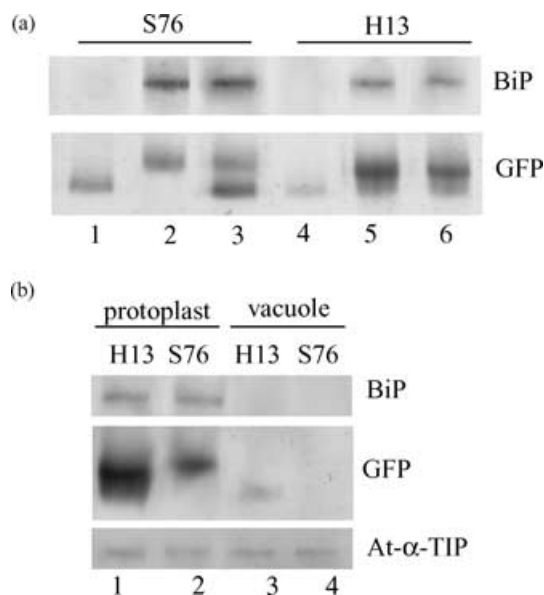


**Figure 4.** secGFP is present in the apoplast in a truncated form.

(a) Immunoblot analysis of proteins extracted from seedlings (lanes 3 and 6), protoplasts (lanes 2 and 5) and the extracellular space (lanes 1 and 4) of transgenic *Arabidopsis* expressing secGFP (lanes 1–3) and GFP-HDEL (lanes 4–6). Lanes 5 and 6 were diluted threefold in comparison to lanes 2 and 5. (b) Immunoblot analysis of proteins extracted from protoplasts (lanes 1 and 2) of the transgenic *Arabidopsis* GFP-HDEL line H13 (lane 1) and secGFP line S76 (lane 2) and a vacuole-enriched fraction (lanes 3 and 4) prepared from the protoplasts of GFP-HDEL line H13 (lane 3) and secGFP line S76 (lane 4).

S76 and H13 were prepared to determine whether secGFP had indeed been secreted to the apoplast.

In protoplast extracts, secGFP appeared as a single band (Figure 4a, lane 2) that co-migrated with the upper secGFP band present in extracts of whole seedlings (Figure 4a, lane 3). secGFP extracted from extracellular spaces of S76 seedlings also appeared to migrate as a single band (Figure 4a, lane 1), but it co-migrated with the C-terminally truncated form of secGFP that was observed in whole seedling extracts. Extracellular extracts contained no detectable BiP, indicating that the sample was not contaminated by intracellular proteins. Thus, none of the truncated form, but all the full-length secGFP, appeared to be intracellular. These data suggested that secGFP is indeed transported into the apoplast, but is efficiently truncated shortly before or after arrival at this location. The apoplastic form therefore represents the major secGFP species at steady state in S76, and the absence of apoplastic fluorescence indicates that it does not fluoresce to a detectable level in this environment.

In the GFP-HDEL line H13, the extracellular extract had relatively little GFP, but a small quantity of the truncated form of GFP-HDEL was detectable (Figure 4a, lane 4). Using BiP as an intracellular marker, it was shown that contamination with intracellular proteins was below the level of detection. This indicated that some GFP-HDEL was exported from the ER to the apoplast and that, as with secGFP, GFP-HDEL transport was associated with truncation. However, in proteins extracted from H13 protoplasts, both the predominant upper band and the minor lower band were observed (Figure 4a, lane 5) in a ratio similar to that seen in whole tissue extracts (Figure 4a, lane 6). These data indicated that, in contrast to secGFP, much of the truncated GFP-HDEL species was located intracellularly.

To investigate the location of this intracellular truncated form of GFP-HDEL, vacuole-enriched fractions were prepared from protoplasts. These vacuole fractions were marked by an *Arabidopsis* tonoplast intrinsic protein (At-α-TIP), but excluded BiP, and contained a single GFP-HDEL band migrating at the same position as the lower band in protoplast extracts (Figure 4b, lane 3), indicating that the truncated form of GFP-HDEL was present in this TIP-enriched vacuolar fraction. In contrast, no secGFP was detectable in At-α-TIP-enriched fractions prepared from line S76 (Figure 4b, lane 4).

#### *Apoplastic secGFP fluorescence is sensitive to environmental pH*

The fractionation data show that secGFP is transported to the apoplast, even though fluorescence of GFP is not readily detected in this location. This could be because of the conditions of the apoplastic environment, for example, a pH that is not conducive to GFP fluorescence, or because the

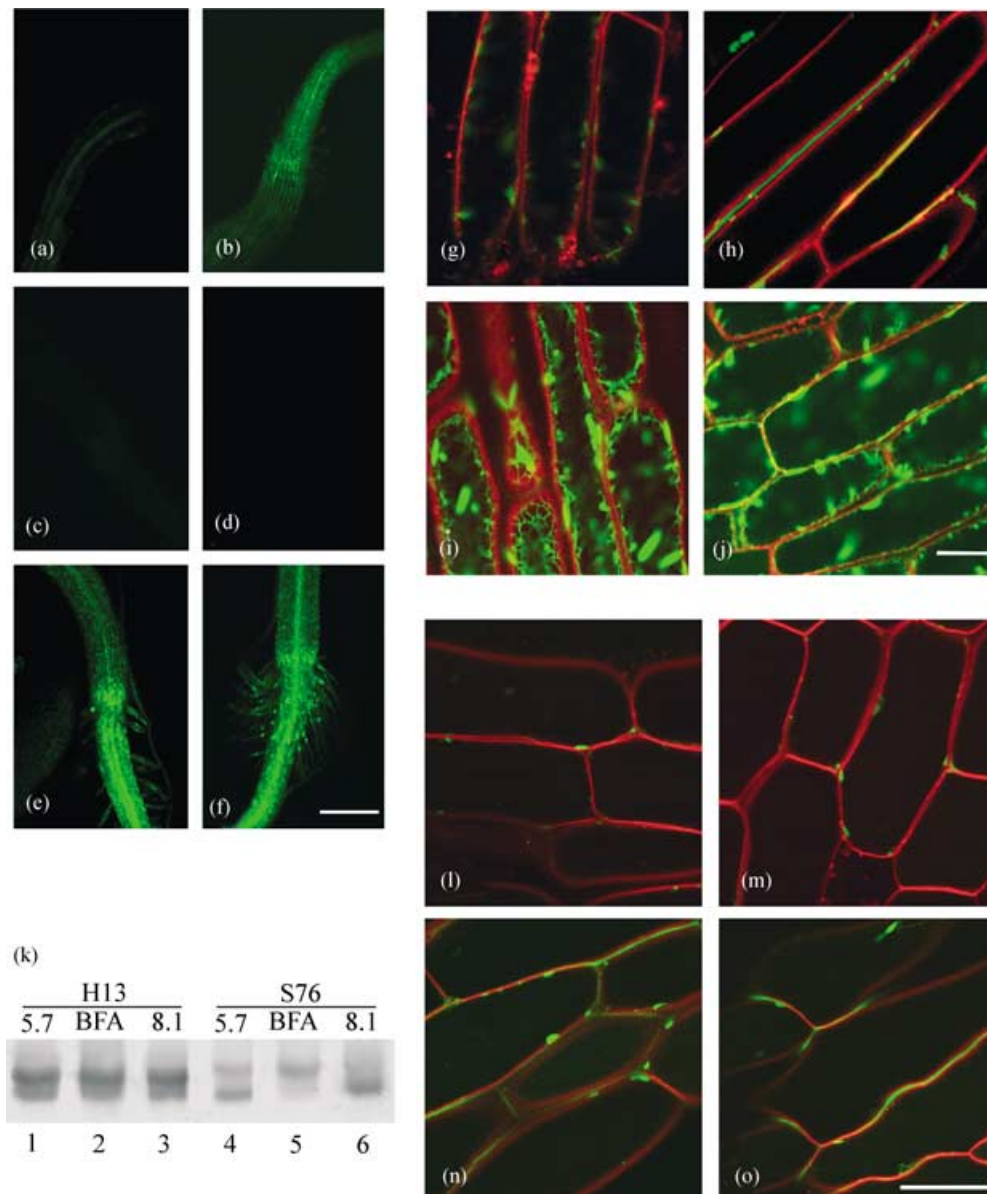


**Figure 5.** Apoplastic secGFP can be fluorescent, but it is sensitive to environmental pH.

(a–f) Low magnification confocal images of GFP fluorescence in secGFP line (a, b), wt (c, d) and GFP-HDEL (e, f) line cultured in MS medium adjusted to pH 5.7 (a, c, e) or pH 8.1 (b, d, f). Bar = 250 μm.

(g–j) Merged confocal laser scanning images of GFP fluorescence and FM4-64 fluorescence in cells of either secGFP (g, h) or GFP-HDEL (i, j) seedlings grown in MS medium having pH 5.7 (g, i) or 8.1 (h, j). Bar = 25 μm.

(k) Immunoblot analysis of protein extracts from GFP-HDEL line H13 (lanes 1–3) and secGFP line S76 (lanes 4–6) incubated in pH 5.7- (lanes 1 and 4) and pH 8.1 (lanes 3 and 6)-buffered MS medium, as well as in BFA (36 μM; lanes 2 and 5). Immunodetection was carried out with anti-GFP.

(l–o) Merged confocal laser scanning images of GFP fluorescence and FM4-64 fluorescence in cells of secGFP line S76 grown at pH 5.7 (l, m) or 8.1 (n, o) in the presence (m, o) or absence (l, n) of cytD. Bar = 25 μm.

truncated form of secGFP, which exists in the apoplast, is not capable of fluorescing. To investigate these possibilities, seedlings of lines S76 and H13 were cultured on MS medium adjusted to pH 8.1 and, as usual, were compared with seedlings grown at pH 5.7. At low magnification, GFP fluorescence was seen to have increased in intensity in S76 seedlings grown at pH 8.1 for 2 days (Figure 5b versus

Figure 5a). In contrast, no clear change in fluorescence was found in either wt *Arabidopsis* (Figure 5d versus Figure 5c) or line H13 (Figure 5f versus Figure 5e), indicating that fluorescence enhancement on media with pH 8.1 was specific to secGFP. Examination by confocal laser scanning microscopy revealed that S76 seedlings cultured at pH 8.1 showed clearly visible secGFP fluorescence in the

apoplastic space as defined by FM4-64 staining of two adjacent PMs (Figure 5h), while those cultured at pH 5.7 exhibited no detectable secGFP in the apoplast (Figure 5g). S76 seedlings cultured at pH 8.1 did not display any change in the intensity or pattern of intracellular fluorescence, indicating that the effect of environmental pH on fluorescence was specific to apoplastic secGFP. In the case of GFP-HDEL line H13, seedlings cultured at pH 8.1 exhibited the same ER-localised GFP distribution as those at pH 5.7, and no apoplastic fluorescence was detectable (Figure 5i,j). The data further suggest that secGFP is transported to the apoplast and it can fluoresce, but its fluorescence is sensitive to the pH of the culture medium surrounding the plants.

To investigate the mechanisms that underlie the enhancement of apoplastic secGFP fluorescence at pH 8.1, proteins extracted from S76 and H13 seedlings that had been grown at each pH were analysed by immunoblotting using GFP antiserum. GFP-HDEL extracted from H13 seedlings grown either at pH 5.7 or 8.1 exhibited identical banding patterns with a predominant upper band and a minor lower band, as described above (Figure 5k, lanes 1 and 3). This is consistent with the lack of any change in GFP-HDEL fluorescence in H13 at pH 8.1, when examined by confocal microscopy. On the other hand, secGFP extracted from S76 seedlings cultured at pH 8.1 showed a small increase in the intensity of the already predominant lower band in comparison to extracts of S76 cultured at pH 5.7 (Figure 5k, lane 6 versus lane 4). This suggests that visible secGFP fluorescence in the apoplast of S76 seedlings cultured at pH 8.1 resulted principally from the truncated lower band, implying that this truncated species can be fluorescent in a suitable environment.

*Treatment with BFA, but not cytochalasin D (cytD), results in enhanced intracellular GFP fluorescence that resembles the ER network*

We next asked whether secGFP transported to the apoplast of S76 seedlings could report on perturbation of intracellular membrane traffic. It has been shown that inhibition of anterograde membrane traffic by BFA in tobacco epidermal cells results in intracellular secGFP accumulation associated with enhanced GFP fluorescence (Batoko *et al.*, 2000; Boevink *et al.*, 1999). To test whether secGFP fluorescence in S76 is also sensitive to BFA, seedlings were incubated with 36  $\mu$ M BFA for periods ranging from 5 h to 2 days, and were subjected to confocal analysis. No clear change in secGFP fluorescence was discernible after 20 h of incubation in BFA, but detectable enhancement of secGFP fluorescence was evident in seedlings incubated in BFA for 25 h or more (Figure 6d versus Figure 6a). No change in the intensity of green fluorescence was observed in wt (Figure 6e versus Figure 6b) or H13 seedlings incubated in BFA for up to 2 days (Figure 6f versus Figure 6c).

Examination at higher magnification revealed that the enhanced GFP fluorescence observed in S76 seedlings in the presence of BFA resulted from enhanced intracellular fluorescence. In contrast to control seedlings, where weak GFP fluorescence was visible only in fusiform bodies (Figure 6g), BFA-treated seedlings imaged with the same parameters exhibited a pattern typical of the ER network along with some small dots and bodies with irregular shapes (Figure 6h). Similarly, in H13 seedlings incubated with BFA, GFP-HDEL marked a typical ER network, but some small dots and some irregular bodies were also seen (Figure 6k versus Figure 6j). Similar small dots have been reported in BFA-treated tobacco epidermal cells transiently expressing secGFP and GFP-HDEL (Batoko *et al.*, 2000).

When proteins were extracted from BFA-treated S76 seedlings and analysed by immunoblotting with GFP antiserum, the upper secGFP band was seen to have increased in intensity at the expense of the lower band (Figure 5k, lane 5 versus lane 4), indicating that secGFP proteolysis is sensitive to BFA action. This is consistent with the proposal that the carboxyl-terminal truncation of secGFP occurs after export from the ER. GFP-HDEL extracted from BFA-treated H13 seedlings exhibited no clear change in the ratio of the two bands (Figure 5k, lanes 1 and 2).

In *Tradescantia* pollen tubes, maize root cap and auxin-stimulated oat coleoptile cells, treatment with the actin de-polymerising drug cytD has been shown to induce accumulation of vesicles around Golgi bodies (Phillips *et al.*, 1988; Shannon *et al.*, 1984). However, in tobacco cells, actin de-polymerisation does not appear to inhibit the transport of membrane markers between the ER and Golgi (Brandizzi *et al.*, 2002; Saint-Jore *et al.*, 2002), even though the mobility of the ER and Golgi is dependent on the actin cytoskeleton (Boevink *et al.*, 1998; Liebe and Quader, 1994; Nebenführ *et al.*, 1999). To determine if disruption of actin filaments by cytD would inhibit secGFP transport leading to enhanced intracellular secGFP fluorescence, seedlings of S76 and H13 were incubated with 39.4  $\mu$ M cytD and the GFP fluorescence and subcellular locations in the treated seedlings were examined. In contrast to BFA treatment, we found no clear difference in secGFP fluorescence intensity and location between cytD-treated (Figure 6i) and non-treated secGFP seedlings (Figure 6g). Cytochalasin-D-evoked disintegration of ER tubules (Liebe and Quader, 1994) was evident in the treated H13 seedlings (Figure 6l). We also noted that all treated seedlings exhibited retarded root and root hair growth, increased radial expansion and wavy root hairs with swollen tips as described previously by Baskin and Bivens (1995), indicating the efficacy of cytD in the treated seedlings (data not shown). When S76 seedlings grown on medium at pH 8.1 were treated with cytD, secGFP was clearly visible in the apoplast, indicating that secGFP can indeed continue to be secreted in the presence of this drug (Figure 5o).

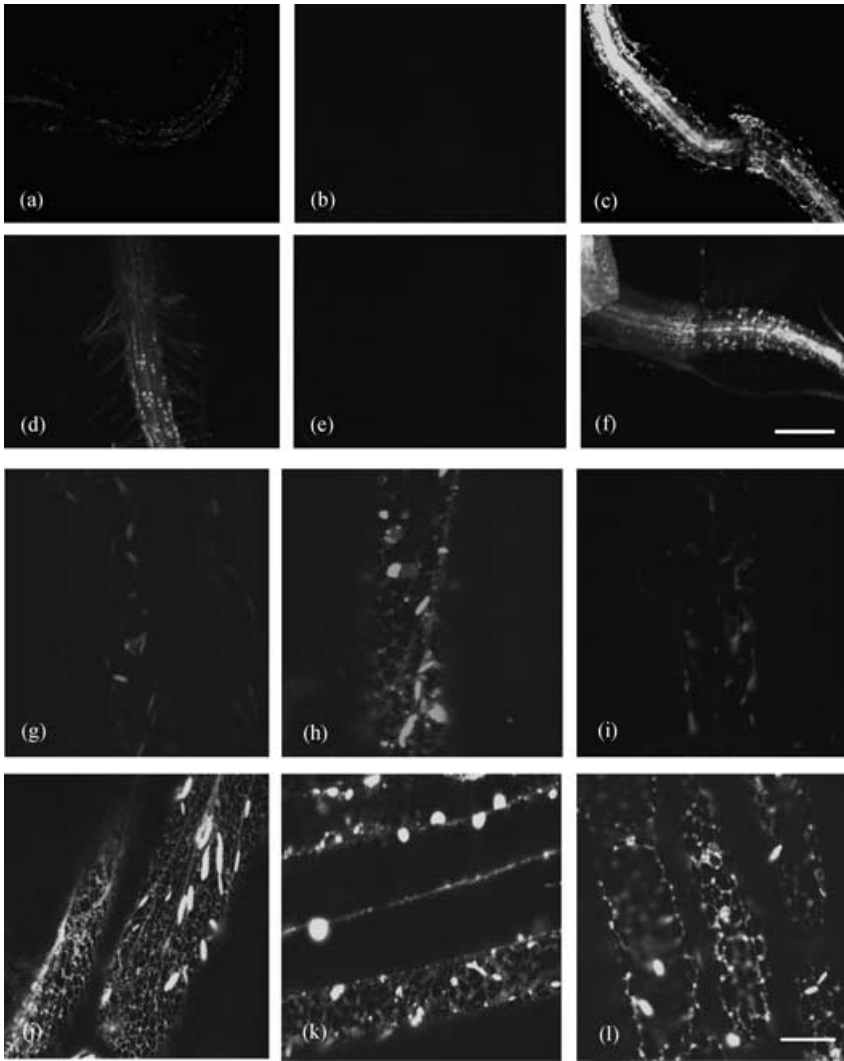


**Figure 6.** Treatment with BFA, but not cytD, results in enhanced intracellular GFP fluorescence that resembles the ER network.

(a–f) Low magnification confocal laser scanning microscopy of GFP fluorescence in secGFP (a,d), wt (b,e) and GFP-HDEL (c,f) seedlings incubated in water (a–c) or BFA (36  $\mu$ M; d–f). Bar = 250  $\mu$ m.

(g–l) Confocal laser scanning images of GFP fluorescence in either secGFP (g–i) or GFP-HDEL (j–l) expressing *Arabidopsis* seedlings incubated in water (g,j), BFA (h,k) or cytD (i,l). Bar = 25  $\mu$ m.

#### *rhd3* has enhanced intracellular secGFP fluorescence and an unusual ER organisation in roots

Data from the molecular characterisation of transgenic lines expressing secGFP indicated that the S76 line may be used as a visual *in vivo* assay for the analysis of inhibitors that perturb protein transport and endomembrane dynamics. To determine whether the system could be used to report on genetic defects that affect membrane traffic, we examined secGFP distribution in *rhd3* (Schieffelbein and Somerville, 1990; Wang *et al.*, 1997). Following an ultrastructural analysis of *rhd3* root hairs, a number of possible roles for RHD3 were postulated, including a role in biosynthetic membrane traffic (Galway *et al.*, 1997). Such a role has not yet been demonstrated, but if RHD3 is required for anterograde vesicle transport, secGFP expression in *rhd3* plants should be accompanied by enhanced intracellular GFP fluorescence relative to wt plants.

Line S76 was crossed with *rhd3-1*, and hygromycin-resistant secGFP *rhd3* seedlings of the F<sub>2</sub> and F<sub>3</sub> generations

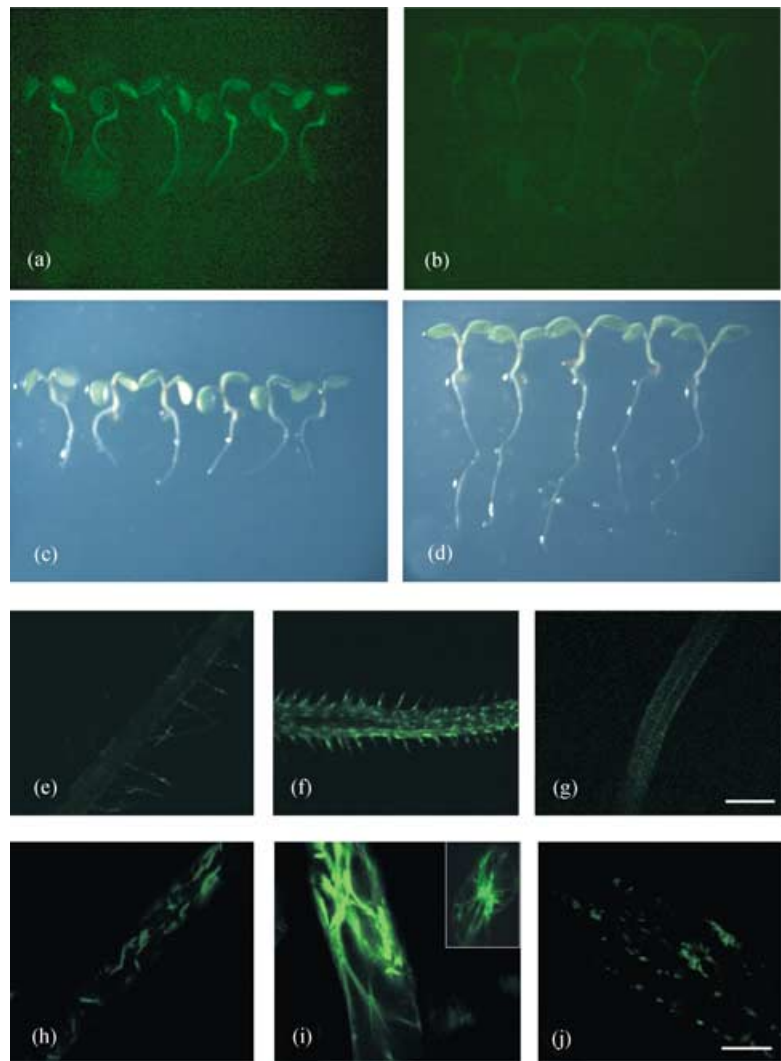
were examined by fluorescence microscopy. At low magnification, detectable enhancement of fluorescence was evident in the roots of secGFP *rhd3* seedlings when compared with *RHD3* sibling S76 (compare Figure 7a and Figure 7b), but no change in GFP fluorescence was apparent in the shoots of secGFP *rhd3* plants. Closer examination by confocal microscopy confirmed the enhancement of secGFP fluorescence in *rhd3* roots (Figure 7f versus Figure 7e). In contrast to *rhd3*, no detectable difference in intensity of GFP fluorescence was observed in seedlings of another root hair mutant *shv1-4* (Parker *et al.*, 2000) crossed with secGFP (compare Figure 7g and Figure 7e). Unlike wt secGFP plants, where GFP was detected only in weakly fluorescent fusiform bodies (Figure 7h), secGFP fluorescence in epidermal cells of *rhd3* plants was readily visible in a reticulate structure in addition to the fusiform bodies (Figure 7i). However, in contrast to the fine meshwork of the cortical ER in wt plants, the network labelled by secGFP in *rhd3* plants had a much coarser cable-like organisation often oriented parallel to the long axis of the cell (Figure 7i).

**Figure 7.** *rh**d3* has enhanced intracellular secGFP fluorescence that marks an unusual cable-like structure in root epidermal cells and root hairs.

(a–d) Fluorescent (a,b) and bright-field (c,d) stereomicrographs of secGFP-expressing *rh**d3* (a,c) and wt seedlings (b,d).

(e–g) Low magnification confocal laser scanning microscopy of GFP fluorescence in roots of secGFP-expressing wt (e), *rh**d3-1* (f) and *shv1-4* (g). Bar = 250  $\mu$ m.

(h–j) Confocal GFP fluorescence micrographs of root epidermal cells of a secGFP expressing wt plant (h), *rh**d3-1* (i) and *shv1-4* (j) mutants. Inset in (i) is a confocal image of GFP fluorescence in a root hair of secGFP-expressing *rh**d3*. Bar = 25  $\mu$ m.



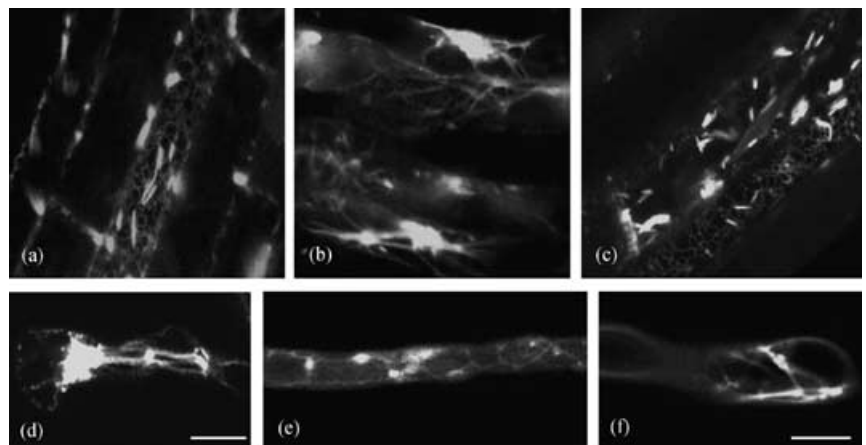
No similar structure was noticed in *shv1-4* plants expressing secGFP (Figure 7j), suggesting that this was not a general feature of mutants with developmentally abnormal root hairs.

When the GFP-HDEL marker in line H13 was introgressed into the *rh**d3* background, GFP-HDEL in root epidermal cells marked structures that were very similar to those that accumulated secGFP, with characteristic cables extending

**Figure 8.** The unusual cable-like structure is related to unusual ER network in root epidermal cells and root hairs of *rh**d3* and it is an intrinsic characteristic of the mutant.

(a–d) Confocal laser scanning fluorescence micrographs of GFP-HDEL in root cells of wt (a), *rh**d3* (b) and *shv1* backgrounds (c), and a root hair of *rh**d3* (d). Bar = 25  $\mu$ m.

(e, f) Confocal laser scanning microscopy of DiOC<sub>6</sub> fluorescence in a root hair of wt (e) and *rh**d3* mutant plant (f). Bar = 25  $\mu$ m.



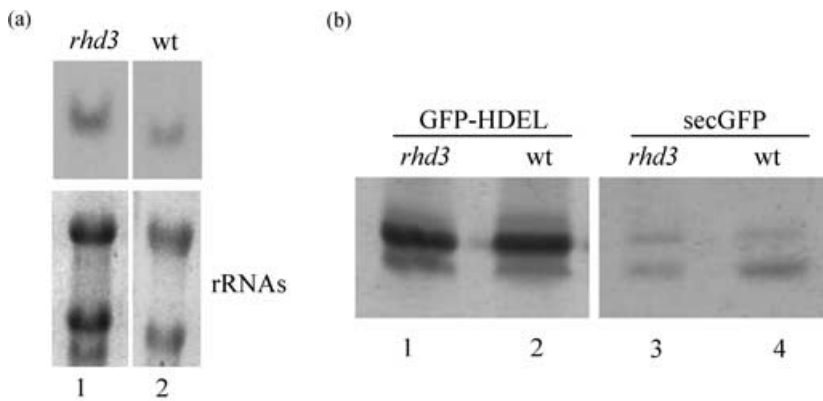


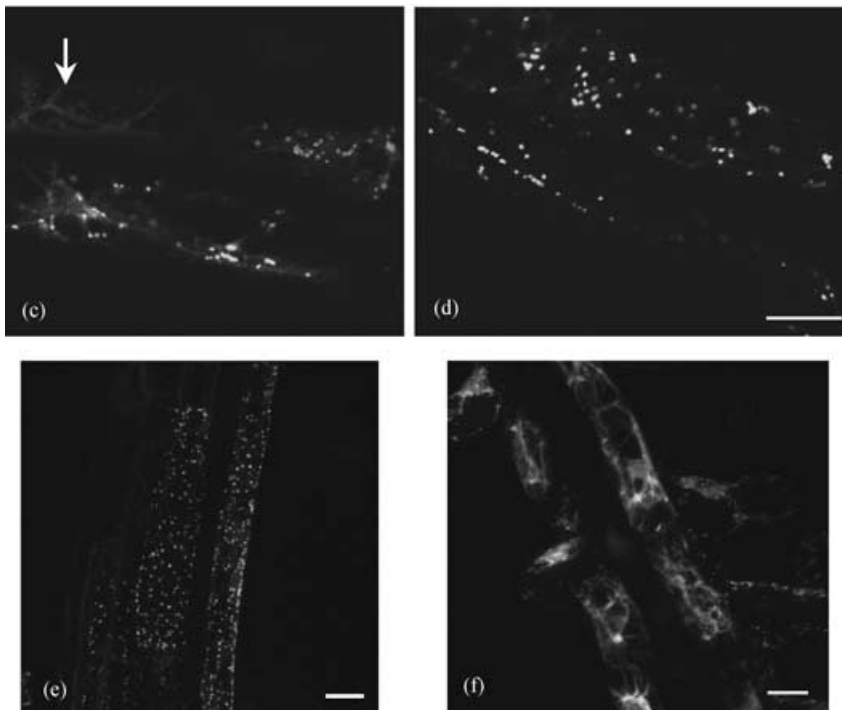
**Figure 9.** Inhibition of the C-terminal proteolysis of secGFP and distribution of ST-GFP in the ER.

(a) RNA blot revealed no apparent difference in steady-state abundance of secGFP mRNA in *rhd3* (lane 1) and wt (lane 2) background.

(b) Immunoblot analysis of secGFP (lanes 3 and 4) and GFP-HDEL (lanes 1 and 2) accumulation in *rhd3-1* (lanes 1 and 3) in comparison to wt (lanes 2 and 4).

(c, d) Confocal images of ST-GFP distribution in *rhd3* (c) and wt (d). Bar = 25  $\mu$ m.

(e, f) Projections of series of confocal images of ST-GFP distribution in wt (e) and *rhd3* (f). Bar = 20  $\mu$ m.



parallel to the long axis of the cells (compare Figure 8b,d to Figure 8a). This suggests that the unusual cable-like structure highlighted by secGFP fluorescence in *rhd3* roots was a disorganised form of the ER. To rule out the possibility that the observed ER disorganisation was caused by accumulation of GFP in the *rhd3* mutant, *rhd3* plants that did not express GFPs were stained with 3,3'-dihexyloxycarbocyanine iodide (DiOC<sub>6</sub>). In the *rhd3* mutant, DiOC<sub>6</sub> fluorescence identified a cable-like network similar to the one revealed by GFP-HDEL (Figure 8f), whereas the dye stained a typical ER network in wt *Arabidopsis* (Figure 8e). This result suggested that the disorganised ER labelled by secGFP and GFP-HDEL was intrinsic to *rhd3*. Such a disorganised ER system was not observed in GFP-HDEL plants homozygous for *shv1-4* (Figure 8c), indicating again that the unusual ER pattern was not a general feature of root hair mutants.

There was no apparent difference in steady-state abundance of secGFP mRNA extracted from wt and *rhd3* (Figure 9a), so the increased intracellular secGFP fluorescence in *rhd3* is unlikely to have resulted from an increased rate of secGFP synthesis. We also investigated whether the ratio of full length to truncated secGFP caused by a BFA-sensitive proteolysis was altered in *rhd3*. Total proteins were extracted from roots of wt and mutant seedlings expressing each marker. There was no detectable alteration in the ratio of the two GFP-HDEL bands in wt and *rhd3* seedlings (Figure 9b, lanes 1 and 2). In the case of secGFP, there appeared to be a slight increase in the ratio of upper to lower bands in *rhd3* extracts in comparison with those from *RHD3* seedlings (Figure 9b, lanes 3 and 4), indicating an increase in the proportion of secGFP that was protected from the C-terminal proteolysis that occurs downstream

of the ER. These observations are consistent with a quantitative reduction in the rate of anterograde transport of secGFP in *rhd3*.

#### *Distribution of ST-GFP in the ER of rhd3*

The enhanced fluorescence of secGFP in the ER and inhibition of secGFP proteolysis in *rhd3* suggested that the mutant might be at least partially defective in protein transport out of the ER. To further test this notion, we examined the intracellular distribution of ST-GFP, a GFP fused with the amino-terminal 52 residues of the rat *trans*-Golgi enzyme sialyltransferase, which targets GFP to the Golgi in plants (Boevink *et al.*, 1998; Saint-Jore *et al.*, 2002). In roots of transgenic *Arabidopsis*-expressing ST-GFP, the fluorescence pattern is typical of Golgi stacks that are scattered throughout cells (Boevink *et al.*, 1998; Saint-Jore *et al.*, 2002; Figure 9d,e). However, in the *rhd3* background, in many root epidermal cells examined, ST-GFP labelled an additional cable-like structure that resembled the disorganised ER that characterises this mutant (Figure 9c). Remarkably, in some cells, no ST-GFP-labelled Golgi stacks, but only the cable-like ER structures (Figure 9c (arrow) and Figure 9f), were visible.

## Discussion

### *The potential of secGFP for the analysis of mutants and gene products involved in endomembrane traffic and organisation in Arabidopsis*

*Arabidopsis* has, for many years, been used as a model plant to elucidate the molecular regulation of biological processes. However, genetic analysis of the secretory pathway in *Arabidopsis* has been hampered by the lack of either simple phenotypic traits that are indicative of secretory defects, or a visual non-invasive secretory marker. In this study, we demonstrate that secGFP, a chimeric GFP fusion (Batoko *et al.*, 2000), when constitutively expressed in *Arabidopsis*, functions as a simple, visual, non-destructive *in vivo* marker that can be used to monitor protein transport and endomembrane dynamics. secGFP exhibits reduced GFP fluorescence in comparison to GFP-HDEL, an ER-resident GFP. secGFP is exported from the ER and transported to the apoplast where its fluorescence is weak. The protein accumulates poorly and is subject to proteolysis at the carboxyl terminus that results in steady-state accumulation of a C-terminal-truncated form in the apoplast. It is not clear where, in the secretory pathway, the carboxyl-terminal proteolysis occurs, but it is reduced in the presence of BFA, so it is most likely a transport-dependent post-ER event. Only full-length protein was detected in protoplasts, while the apoplast contained only the truncated form, so

proteolysis probably occurs shortly before or soon after delivery to the apoplast.

Fluorescence of GFP has been shown to tolerate loss of 12 amino acid residues at the carboxyl terminus (Li *et al.*, 1997), and such a deletion would produce a species similar in size to the truncated apoplastic form of secGFP. Our data suggest that the carboxyl-terminal truncation in secGFP is unlikely to be the major reason that secGFP seedlings exhibit weak fluorescence, because seedlings grown at pH 8.1 exhibited increased apoplastic GFP fluorescence accompanied by an increase in the abundance of the truncated form. Thus, it seems likely that the truncated form can fluoresce, but that the apoplastic environment does not favour the accumulation or fluorescence of this molecule. Tamura and colleagues have recently reported very similar observations with vacuolar-targeted GFP in *Arabidopsis* (Tamura *et al.*, 2003). These authors found that a pH-dependent carboxyl-terminal processing event occurs shortly after GFP arrives in vacuoles of light- or dark-grown *Arabidopsis* seedlings, followed by rapid light-dependent degradation. However, growth of seedlings in the dark or inhibition of vacuolar H<sup>+</sup>-ATPase activity resulted in a marked increase in the stability of the truncated form with a concomitant increase in vacuolar fluorescence (Tamura *et al.*, 2003). In case of apoplastic secGFP, it appeared that under alkaline culture conditions, the turnover of the truncated secGFP in the apoplast was slow, leading to an increase in secGFP protein accumulation. Such an increase might contribute to the enhancement of apoplastic secGFP fluorescence. We do not know the apoplastic pH in roots of secGFP seedlings growing at pH 5.7 and 8.1, and we cannot determine the relative contributions of increased protein accumulation and increased GFP brightness to the enhancement of apoplastic GFP fluorescence at pH 8.1. GFP fluorescence is known to be pH-sensitive (Tsien, 1998), and the pK<sub>a</sub> of mGFP5 was reported to be similar to that of wtGFP, which is near 4.5 (Liu *et al.*, 2001; Tsien, 1998). The pH of the apoplast is generally believed to be lower than that of most intracellular compartments, and estimates of apoplastic pH in maize roots cultured hydroponically are typically in the range of 4.8–5.3, depending on external growth solutions (Kosegarten *et al.*, 1999). Consequently, apoplastic secGFP in *Arabidopsis* might be capable of fluorescence, but under routine culture conditions, its intensity might be compromised. Alternatively, if secGFP molecules are secreted to the apoplast before they have acquired fluorescence, they may become fluorescent at a slow rate relative to their turnover in this environment.

### *How does a minor portion of GFP-HDEL escape from the ER?*

In this study, a minor portion of the GFP-HDEL protein was found in a vacuolar compartment, as well as in the apoplast.

Previous studies have also reported loss of artificial HDEL-containing proteins from the ER of transgenic plants (Gomord *et al.*, 1997; Herman *et al.*, 1990), and at least one protein containing the ER tetrapeptide Lys-Asp-Glu-Leu (KDEL), auxin-binding protein (ABP), has also been found to be secreted at low levels (Jones and Herman, 1993). One possible explanation for GFP-HDEL escape from the ER is saturation of the K/HDEL receptor that can lead to the protein entering the anterograde bulk flow pathway to the apoplast (Crofts *et al.*, 1999). Second, the efficiency with which the HDEL signal is recognised can be influenced by local sequence and structural features (Denecke *et al.*, 1992); therefore, it is possible that the HDEL signal is presented suboptimally in GFP-HDEL. Another alternative possibility is that the C-terminal proteolysis, which removes the HDEL signal, occurs in the Golgi. Any one of the above mechanisms could account for the small portion of GFP-HDEL that accumulates in the apoplast of H13 at steady state; however, the predominant location of the truncated form is a vacuole. It may be that GFP-HDEL contains a cryptic vacuolar sorting determinant that results in escaped protein entering one of the vacuolar sorting pathways as reported for GFP in yeast (Kunze *et al.*, 1999). Alternatively, Toyooka *et al.* (2000) demonstrated that sulfhydryl-endopeptidase (SH-EP), a vacuolar cysteine proteinase possessing a C-terminal KDEL sequence, was transported to protein storage vacuoles via ER-derived granules or vesicles of 0.2–0.5  $\mu\text{m}$ , which bypassed the Golgi. It was proposed that this ER-derived vacuolar ontogenesis might be common in storage tissues of young seedlings (Chrispeels and Herman, 2000). If this pathway operates in some or all cells of the *Arabidopsis* seedlings, GFP-HDEL could be exported to the vacuolar compartment from the ER by such an alternative pathway. It has also been reported that the spindle-shaped fusiform bodies, labelled by GFP-HDEL, selectively accumulate a KDEL protein  $\beta$ -glucosidase and might fuse with vacuoles in response to stress conditions (Matsushima *et al.*, 2003). This might also explain the leakage of GFP-HDEL to vacuolar fractions. Indeed, we found that the abundance of the truncated form of GFP-HDEL was not significantly affected by incubation in BFA for up to 48 h. One explanation for this is that transport to the vacuole occurs via a BFA-insensitive Golgi-independent route. We cannot discount the simpler hypothesis that the truncated form is stable in the vacuole over the course of our BFA treatment, even though the apoplastic form is not. However, this possibility seems less likely following the recent report that vacuolar GFP is rapidly degraded via a light-dependent mechanism that would be expected to operate during the 16-h photoperiod used in our experiments (Tamura *et al.*, 2003).

Although we were able to detect increased intracellular accumulation of secGFP in *Arabidopsis* root epidermal cells treated with BFA, it took more than 20 h for this to become apparent. In contrast, BFA-induced changes in the

distribution of PIN proteins in *Arabidopsis* root tips and embryos occur within minutes (Geldner *et al.*, 2001, 2003; Steinmann *et al.*, 1999). This discrepancy must, in part, reflect the time taken for sufficient new secGFP to accumulate, following inhibition of anterograde traffic in our assay. Yet, during transient expression of secGFP in tobacco leaf epidermal cells, secGFP accumulation was evident 4–6 h after BFA treatment (Batoko *et al.*, 2000). While it is possible that the rate of secGFP synthesis is higher in the tobacco transient expression system, BFA seems to be a less potent (and possibly indirect) inhibitor of anterograde traffic in *Arabidopsis* root epidermal cells than it is of endocytic recycling in *Arabidopsis* root tips or of anterograde traffic in tobacco leaf epidermal cells. It was reported recently that anterograde traffic of a PM marker was unperturbed by short-term treatment of *Arabidopsis* root tips with 50  $\mu\text{M}$  BFA, although endocytic recycling was rapidly affected (Grebe *et al.*, 2003). Furthermore, BFA causes Golgi markers to cluster around BFA bodies in *Arabidopsis* root tips, rather than to fuse with the ER as in tobacco leaf epidermis (Boevink *et al.*, 1998; Grebe *et al.*, 2003; Saint-Jore *et al.*, 2002). Geldner *et al.* (2003) have pointed out that *Arabidopsis* has eight ARF-GEFs (the targets of BFA) that differ in their sensitivity to BFA and probably also differ in their sites of action in the cell, as well as their distributions in various tissues. Consequently, differences in the reported effects of BFA are likely to reflect the differing sensitivities of the ARF-GEFs involved in anterograde and endocytic traffic in each cell type of a particular species.

#### *RHD3 is required for anterograde membrane traffic and normal ER structure*

The secGFP line is an attractive tool for genetic and transgenic analysis of genes that might interfere with membrane traffic in the plant secretory pathway. The behaviour of secGFP in BFA-treated seedlings suggested that by analysis of the intensity and distribution of secGFP fluorescence coupled with an analysis of secGFP processing, gene products involved in membrane traffic, at least from the ER to the Golgi, could be identified. We confirmed this by introducing secGFP into a known mutant line, *rhd3*, and identified a requirement for RHD3 function in ER–Golgi traffic and ER organisation.

*rhd3* was shown to be defective in cell expansion in root hairs and epidermal cells (Wang *et al.*, 1997). Ultrastructural analysis of its root hairs revealed an abnormal distribution of vesicles in the subapical region and altered vacuole organisation (Galway *et al.*, 1997). Based on this, roles for RHD3 in some aspect of membrane trafficking, ionic homeostasis or vacuole function have been postulated, but none has been demonstrated. Here, we show that RHD3 is required for normal secGFP export from the ER

and for normal ER organisation in roots. Furthermore, the Golgi marker ST-GFP, which normally exhibits an exclusively punctate labelling of the Golgi stacks (Boevink *et al.*, 1998; Saint-Jore *et al.*, 2002), was found to accumulate in the disorganised ER of *rhd3* root hairs and epidermal cells. These observations suggest that RHD3 is required for normal anterograde traffic between the ER and Golgi. It is very likely that the deficiency in ER–Golgi traffic is partial: the fluorescence of secGFP in *rhd3* was substantially lower than that of GFP-HDEL, the reduction in transport-dependent processing of secGFP was lower than that induced by BFA and *rhd3* root hairs continued to grow at about half the rate of wt (Galway *et al.*, 1997). Furthermore, efficient inhibition of ER–Golgi traffic is expected to result in cell death. Thus, our data demonstrate that the secGFP assay is able to identify sublethal quantitative reductions in the rate of anterograde membrane traffic.

In support of our conclusions, it is interesting to note that the yeast homologue of RHD3, Sey1p, is a synthetic enhancer of Yop1p (Brands and Ho, 2002). Yop1p is an integral Golgi membrane protein involved in biosynthetic membrane traffic in conjunction with Yip1p (Calero *et al.*, 2001), which is another integral membrane protein that is packaged into ER-derived vesicles, required for ER–Golgi vesicle fusion and interacts with the Rab GTPases Ypt1p and Ypt31p/32p (Barrowman *et al.*, 2003; Yang *et al.*, 1998). Ypt1p is required for ER–Golgi and intra-Golgi traffic in yeast, while Ypt31p/32p is required for export from the *trans*-Golgi compartment, where secretory, Golgi-resident and vacuolar proteins are sorted into distinct membrane vesicles (Ortiz *et al.*, 2002). A role for RHD3 in facilitating Rab GTPase function on the Golgi in *Arabidopsis* could account for the diverse phenotypes in cell growth, ER–Golgi traffic and vacuole organisation. It is known that *rhd3* root hairs exhibit an abnormal distribution of vesicles in the subapical region (Galway *et al.*, 1997). It will be of interest to identify the origin of these vesicles and to investigate possible genetic interactions between RHD3 and the four Ypt1p homologues or the 26 Ypt31p/32p homologues in *Arabidopsis* (Rutherford and Moore, 2002). The abnormal organisation of the ER network could also be a consequence of impaired ER–Golgi transport in the mutant. In fact, one of the effects of dominant negative Yop1 or Yip1 mutant is abnormal ER membrane structure (Calero *et al.*, 2001; Yang *et al.*, 1998).

We found that the abnormally bundled ER of *rhd3* was also closely associated with actin filaments throughout the length of the root hair and epidermal cells (data not shown). According to Galway *et al.* (1997), cytoskeletal organisation in *rhd3* was not significantly different from the wt; however, vesicles in the subapical region of *rhd3* root hairs were often found aligned along bundled actin filaments in this region. In plants, the mobility of both the ER and the Golgi is

dependent on the actin cytoskeleton (Boevink *et al.*, 1998; Brandizzi *et al.*, 2002; Liebe and Quader, 1994; Nebenführ *et al.*, 1999). Furthermore, in rapidly growing *Tradescantia* pollen tubes, maize root cap cells and auxin-stimulated oat coleoptile cells, de-polymerisation of the actin cytoskeleton led to a rapid accumulation of vesicles around Golgi (Phillips *et al.*, 1988; Shannon *et al.*, 1984). Therefore, one possible role for RHD3 could be to mediate interactions between the endomembrane system and the actin cytoskeleton.

Nevertheless, we think it is unlikely that RHD3 functions primarily or solely in actin-based motility *per se*. First, we did not observe any clear difference in the mobility of the ER, the spindle-bodies or the Golgi stacks in *rhd3*, although the aberrant morphology of these structures made direct comparison difficult. Second, although ER and Golgi membranes each move on actin filaments, de-polymerisation of the actin network in tobacco has no observable effect on the rate of GFP-marker transport to the Golgi (Brandizzi *et al.*, 2002) or on the rate at which Golgi membrane markers fuse with the ER and re-emerge following BFA application and wash-out (Saint-Jore *et al.*, 2002). Finally, treatment of secGFP seedlings with cytD did not cause a clear increase in intracellular secGFP fluorescence as in *rhd3*. As secGFP was also found to accumulate in the apoplast of cytD-treated seedlings grown at pH 8.1, it appears that disruption of actin networks and actin-based motility does not lead to significant reduction in trafficking of secGFP from ER to PM of *Arabidopsis* seedlings under our conditions. A recent study used fluorescence recovery after photobleaching (FRAP) to investigate the trafficking of a GFP marker to the PM, and also concluded that cytD had no effect on this pathway, although endocytic traffic was perturbed (Grebe *et al.*, 2003). It has also been reported that treatment with cytD had little impact on the steady-state distribution of PIN1 in *Arabidopsis* roots (Geldner *et al.*, 2001). The discrepancy between the results obtained in *Arabidopsis* roots and those obtained in pollen tubes, maize root cap and oat coleoptile cells (Phillips *et al.*, 1988; Shannon *et al.*, 1984) may reflect the differing assay systems used or differing requirements for actin networks in each system.

We found that the dye FM4-64 took roughly two times as long to be internalised from the PM and to label internal compartments in *rhd3* seedlings compared to wt (data not shown). This dye has been shown to label vacuoles and pre-vacuolar/endosomal compartments that accumulate recycling PM proteins (Geldner *et al.*, 2003). The reduced uptake of FM4-64 in *rhd3* raises the possibility that *rhd3* is defective in transport from the PM to the vacuole. However, the reduced rate of FM4-64 uptake could easily arise secondarily from a primary defect in anterograde traffic, with the associated reduction in root hair growth, resulting in reduced rates of membrane recycling.

With regard to the primary function of RHD3 in membrane traffic, another possibility is that the cable-like ER structure of *rhd3* might be the first manifestation of the phenotype that secondarily influences transport to the Golgi. In animal cells, Dreier and Rapoport (2000) demonstrated that the formation of the ER network is a controlled vesicle fusion process. If a similar ER network formation model applies to *Arabidopsis*, it is possible that RHD3 might be a factor required for vesicle fusion during the extension of the ER network. Defects in this process could lead to loss of the typical network in *rhd3* and to an accumulation of vesicles associated with actin/bundled ER tubules in the organelle-rich subapical region of root hairs (Galway *et al.*, 1997).

Wang *et al.* (2002) reported that *rhd3* plants exhibit reduced cell expansion in shoot tissues, as well as in root tissues, suggesting that RHD3 may be required throughout *Arabidopsis* development. However, in our studies, *rhd3* shoot tissues did not exhibit clearly enhanced secGFP accumulation. The reason for this is currently unclear, but it is possible that secGFP is not expressed at a level that can reveal the membrane traffic defects in *rhd3* shoots. However, *rhd3* shoot tissues also lacked the clearly abnormal ER organisation and Golgi marker distribution that characterised the roots, so it seems possible that the impairment of membrane traffic in the *rhd3* shoots is not as strong as in the roots. In this regard, it is noteworthy that although the *rhd3* gene is expressed throughout the *Arabidopsis* plant, the primary tissue of its expression might be roots (Wang *et al.*, 2002), and there are two other putative RHD3 homologues in the genome that could have overlapping function in the shoot. It is also notable that young *rhd3* seedlings growing *in vitro* for use in our studies were not readily distinguishable from wt on the basis of their shoot morphology, although roots were obviously shorter. Although the shoot growth phenotype (Wang *et al.*, 1997, 2002) was pronounced in older plants under greenhouse conditions, its penetrance was low in the shoot of seedlings growing *in vitro* under our conditions.

In summary, secGFP provides a simple non-invasive assay for membrane traffic in plants that can identify sublethal, quantitative reductions in anterograde traffic and provide morphological information about the endomembrane compartments affected. It should be possible to use the S76 line in forward screens to identify new mutations in endomembrane traffic and organisation. Indeed, in two screens of EMS-mutagenised M<sub>2</sub> seedlings of the S76 line, we have identified numerous seedlings with increased intracellular secGFP accumulation in a variety of subcellular structures accompanied by a range of seedling lethal and developmental phenotypes (H. Zheng, A. de Kerchove, unpublished). These potentially new membrane trafficking mutants are being characterised genetically and ultrastructurally.

## Experimental procedures

### Plant materials and growth conditions

Transgenic *Arabidopsis* lines expressing secGFP and GFP-HDEL were generated by *Agrobacterium*-mediated transformation of plasmids pVKH18-secGFP and pVKH18-GFP-HDEL (Batoko *et al.*, 2000) into *Arabidopsis* plants (ecotype Columbia-0) using vacuum infiltration (Bent *et al.*, 1994). The freshly prepared infiltration medium (1 l) was: 2.2 g MS salt; 1× B5 vitamins (1000× (100 ml): nicotinic acid (100 mg), thiamine-HCl (1 g), pyridoxine-HCl (100 mg), glycine (200 mg)); 50 g sucrose; 0.044 μM benzylaminopurine (pH 5.7); 200 μl Silwet-77 (Lehle Seeds, USA, Catalog vis-01). Transgenic plants were selected on an MS medium (2.2 g l<sup>-1</sup> MS salt (pH 5.7), 0.8% agar) containing 15 μg ml<sup>-1</sup> hygromycin (Calbiochem, USA). Transgenic *Arabidopsis* homozygous for ST-GFP was made available by Claude Saint-Jore (Oxford, UK). Mutant allele *rhd3-1* was obtained from the *Arabidopsis* stock center (<http://nasc.nott.ac.uk>). Mutant allele *shv1-4* was kindly provided by C. Grierson (Bristol, UK). Introgressions of secGFP and GFP-HDEL into mutant alleles *rhd3-1* and *shv1-4*, and ST-GFP into *rhd3-1*, were carried out by crossing transgenic *Arabidopsis* homozygous for the GFP fusions (pollen donors) with *rhd3-1* and *shv1-4*. Plants were grown either on soil or on the MS medium at 20–22°C under a 16-h photoperiod.

### pH 8.1, BFA and cytochalasin D treatments

For pH 8.1 treatment, *Arabidopsis* seedlings grown on MS medium (pH 5.7) for 4–7 days were transferred onto MS medium adjusted to pH 8.1 with KOH (1N) for further growth. BFA and cytD treatments were performed by growing *Arabidopsis* seedlings in small Petri dishes (Iwaka, Japan) containing either 3 ml solution of BFA (36 μM) or cytD (39.4 μM). Seedlings were first grown on MS plates for 7–21 days before the drug treatments.

### FM4-64 and DiOC<sub>6</sub> staining

*Arabidopsis* seedlings from either pH 5.7- or pH 8.1-buffered MS media were immersed in 3 ml FM4-64 (8.2 μM) in a small Petri dish for 10 min for PM staining. For DiOC<sub>6</sub> staining, 7-day-old *rhd3* and wt seedlings from MS plates were immersed into DiOC<sub>6</sub> solution (1.8 μM) for 30 min.

### Fluorescence stereo and confocal laser scanning microscopy

Intensity of GFP fluorescence in all seedlings was monitored with a fluorescence stereo microscope (Leica, Germany), and all images were captured with a digital camera (Photometrics CoolSnap, Roper Scientific, Marlow, UK). The filter set used was either GFP1 or GFP3. The subcellular localisation of GFP fluorescence, FM4-64 and DiOC<sub>6</sub> staining in seedlings were examined with a confocal laser scanning microscope (Carl Zeiss, LSM 410 or LSM510, Germany). The excitation wavelength for GFP and DiOC<sub>6</sub> was 488 nm and emitted fluorescence was collected with either 510–525 or 505–530 nm band-pass filter. FM4-64 was excited with a 543-nm argon ion laser line and a 580-nm long-pass emission filter. All confocal images obtained were processed with LSMdummy 3.92 (Zeiss, Germany) and PHOTOSHOP 3.0 (Adobe, San Jose, CA, USA) software.

### Protein extraction

Approximately 200 mg of plant material from whole seedlings, roots or shoots were ground in liquid nitrogen and then homogenised in 2× (w/v) protein extraction buffer (75 mM Tris (pH 6.8), 1 mM EDTA, 2% SDS, 3% β-mercaptoethanol, 1 mM phenylmethylsulfonyl fluoride (PMSF)). The homogenates were centrifuged for 5 min at 13 000 *g* to remove plant debris. Proteins in supernatants were precipitated in 6% trichloroacetic acid (TCA) (20 min on ice followed by 15 min centrifugation at 14 000 *g*) and were washed two times with acetone and one time with 100% ethanol. Pellets were completely dried in air and then dissolved in one volume of 1× SDS loading buffer (50 mM Tris-HCl (pH 6.8), 100 mM dithiothreitol (DTT), 2% SDS, 0.1% bromophenol blue, 10% glycerol).

### Subcellular fractionation

Extracellular proteins were extracted according to Monroe *et al.* (1999). To extract proteins from protoplasts, 7-day-old seedlings were briefly rinsed with MM buffer (0.4 M mannitol, 20 mM 2-[*N*-morpholino]ethanesulfonic acid (MES) (pH 5.8)) and cut into small pieces with a sharp blade. The cut *Arabidopsis* pieces were then put into MM buffer containing 1% cellulase 'Onozuka' RS (Yakult Honsha, Tokyo) and 0.1% pectolyase (Sigma, UK). Digestion was allowed for 2 h at room temperature. Protoplasts were filtered through a microcloth (Calbiochem) and washed five times with MM buffer. Pelleted protoplasts were re-suspended in protein extraction buffer and lysed through three consecutive freezing (liquid nitrogen)/thawing cycles. For vacuolar protein extraction, vacuoles were first isolated according to Sansebastiano *et al.* (1998) and were briefly centrifuged and re-suspended in protein extraction buffer and lysed through three consecutive freezing (liquid nitrogen)/thawing cycles. All extracted proteins were then precipitated with 6% TCA and dissolved in 1× SDS-PAGE loading buffer for SDS-PAGE analysis.

### Immunoblot analysis

Protein samples were first separated on a 12% polyacrylamide gel and then electro-transferred onto a nitrocellulose membrane. Protein detection was carried out using the ProtoBlot Western Blot AP system (Promega, Southampton, UK) according to instructions provided by the manufacturer, with several modifications. Non-specific binding sites were first blocked for 1 h with 10% non-fat milk in PBS (pH 7.4; Sigma P3813). The concentrations of primary antibodies were: rabbit anti-*c-myc*, 1 : 1000; rabbit anti-GFP, 1 : 2000; rabbit anti-GFPN15, 1 : 2000; chicken anti-At-α-TIP, 1 : 500; rabbit anti-GRP78(BiP), 1 : 1000. The concentration of alkaline phosphatase-conjugated secondary antibodies (goat antirabbit IgG or antichick IgG) was 1 : 5000. Rabbit antiserum against GFP (anti-GFP, A6455) was purchased from Molecular Probes (Eugene, USA). Rabbit antibody against GFP C-terminal peptides (anti-GFPN15, ab290-100) was purchased from ABCam (Cambridge, UK). Rabbit anti-*c-myc* (A14, sc-789) was purchased from Autogen Bioclear (Calne, UK). Rabbit anti-GRP78(BiP) (Cat. PA1-014) was purchased from Affinity BioReagents (Golden, USA). Chicken anti-At-α-TIP was kindly made available by T. Schaeffner (Muenchen, Germany). All secondary antibodies used in this study were purchased from Promega.

### RNA extraction and gel blot analysis

*Arabidopsis* plant materials of approximately 200 mg were ground in liquid nitrogen and then homogenised in 400 μl GTC buffer (4 M

guanidium thiocyanate, 25 mM sodium citrate (pH 7.0), 0.5% lauryl sarcosine) with freshly added β-mercaptoethanol at 7 μl ml<sup>-1</sup>. The mixture was vortexed for 1 min, followed by addition of 40 μl 2 M NaOAc (pH 4.0), 400 μl phenol (pH 7.0) and vortexing for 1 min. The mixture was shaken for 30 min prior to addition of 80 μl chloroform/isoamyl alcohol (24 : 1) and was then incubated on ice for 15 min, followed by centrifugation at 13 000 *g* at 4°C for 20 min. The water phase (approximately 450 μl) separated was transferred into a new tube, and the same volume of isopropanol was added into the water phase. The mixture was incubated at -20°C for 15 min, followed by centrifugation at 13 000 *g* at 4°C for 15 min. The pellet was dried in air and was then dissolved with 300 μl GTC with freshly added β-mercaptoethanol at 7 μl ml<sup>-1</sup>. The suspension was spun for 5 min at 13 000 *g*, and the supernatant was transferred into a new tube followed by addition of the same volume of isopropanol. The mixture was incubated at -20°C for 15 min followed by centrifugation at 13 000 *g* at 4°C for 15 min. The RNA pellet was washed with 80% ethanol, air dried and dissolved in 20–60 μl de-ionised formamide. For gel blot analysis, approximately 10 μg RNA per lane was separated on a 1.1% denaturing agarose gel, transferred onto a nylon membrane and hybridised with <sup>32</sup>P-labelled GFP DNA followed by detection by autoradiography (Figure 9) or phosphorimaging (Figure 3).

### Acknowledgements

We are grateful to Tony Schaeffner, GSF Research Centre, Muenchen, Germany for antibodies to At-α-TIP; Claire Grierson, University of Bristol, UK, for seeds of *shv1-4*; Claude Saint-Jore, Oxford Brookes University, for generating the ST-GFP *Arabidopsis* line and Jim Haseloff, University of Cambridge, UK, for mGFP5. We thank Alexis de Kerchove for the analysis of secGFP transcript levels in *rhd3* and *RHD3* backgrounds. This work was supported by an Oxford Brookes Studentship award to H.Z. and Biotechnology and Biological Sciences Research Council grants to I.M. and C.H. In a recently published paper (Hu *et al.*, 2003), it is shown that *fragile fibre 4* is allelic to *rhd3*. Immunofluorescence labelling of *fra4* revealed that actin was bundled into thick cables in elongating root epidermal cells though cortical microtubules appeared normal. These observations are consistent with the abnormal ER organisation we report for *rhd3*. Furthermore, the cell wall biosynthesis defect of *fra4* is consistent with our finding that *rhd3* is defective in biosynthetic membrane traffic and in Golgi marker localisation.

### References

- Ahmed, S.U., Rojo, E., Kovaleva, V., Venkataraman, S., Dombrowski, J.E., Matsuoka, K. and Raihkel, N.V. (2000) The plant vacuolar sorting receptor AtELP is involved in transport of NH<sub>2</sub>-terminal propeptide-containing vacuolar proteins in *Arabidopsis thaliana*. *J. Cell. Biol.* **149**, 1335–1344.
- Assaad, F.F., Huet, Y., Mayer, U. and Jurgens, G. (2001) The cytokinesis gene *KEULE* encodes a Sec1 protein that binds the syntaxin KNOLLE. *J. Cell Biol.* **152**, 531–543.
- Barrowman, J., Wang, W., Zhang, Y. and Ferro-Novick, S. (2003) The Yip1p–Yif1p complex is required for fusion competence of endoplasmic reticulum-derived vesicles. *J. Biol. Chem.* **278**, 19878–19884.
- Baskin, T.I. and Bivens, N.J. (1995) Stimulation of radial expansion in *Arabidopsis* roots by inhibitors of actomyosin and vesicle secretion but not by various inhibitors of metabolism. *Planta*, **197**, 514–521.

- Batoko, H., Zheng, H.Q., Hawes, C. and Moore, I. (2000) A Rab1 GTPase is required for transport between the endoplasmic reticulum and Golgi apparatus and for normal Golgi movement in plants. *Plant Cell*, **12**, 2201–2218.
- Bent, A.F., Kunkel, B.N., Dahlbeck, D., Brown, K.L., Schmidt, R., Giraudat, J., Leung, J. and Staskawicz, B.J. (1994) *RPS2* of *Arabidopsis thaliana*: a leucine-rich repeat class of plant disease resistance genes. *Science*, **265**, 1856–1860.
- Boevink, P., Oparka, K., Santa Cruz, S., Martin, B., Betteridge, A. and Hawes, C. (1998) Stacks on tracks: the plant Golgi apparatus traffics on an actin/ER network. *Plant J.* **15**, 441–447.
- Boevink, P., Martin, B., Oparka, K.J., Santa Cruz, S. and Hawes, C. (1999) Transport of virally expressed green fluorescent protein through the secretory pathway in tobacco leaves is inhibited by cold shock and Brefeldin A. *Planta*, **208**, 392–400.
- Bogdanove, A.J. and Martin, G.B. (2000) AvrPto-dependent Pto-interacting proteins and AvrPto-interacting proteins in tomato. *Proc. Natl. Acad. Sci. USA*, **97**, 8836–8840.
- Bolte, S., Schiene, K. and Dietz, K.J. (2000) Characterization of a small GTP-binding protein of the rab 5 family in *Mesembryanthemum crystallinum* with increased level of expression during early salt stress. *Plant Mol. Biol.* **42**, 923–936.
- Brandizzi, F., Snapp, E.L., Roberts, A.G., Lippincott-Schwartz, J. and Hawes, C. (2002) Membrane protein transport between the endoplasmic reticulum and the Golgi in tobacco leaves is energy-dependent but cytoskeleton-independent: evidence from selective photobleaching. *Plant Cell*, **14**, 1293–1309.
- Brands, A. and Ho, T.H. (2002) Function of a plant stress-induced gene, HVA22. Synthetic enhancement screen with its yeast homolog reveals its role in vesicular traffic. *Plant Physiol.* **130**, 1121–1131.
- Calero, M., Whittaker, G.R. and Collins, R.N. (2001) Yop1p, the yeast homolog of the polyposis locus protein 1, interacts with Yip1p and negatively regulates cell growth. *J. Biol. Chem.* **276**, 12100–12112.
- Cheung, A.Y., Chen, C.Y., Glaven, R.H., de Graaf, B.H., Vidali, L., Hepler, P.K. and Wu, H.M. (2002) Rab2 GTPase regulates vesicle trafficking between the endoplasmic reticulum and the Golgi bodies and is important to pollen tube growth. *Plant Cell*, **14**, 945–962.
- Chrispeels, M.J. and Herman, E.M. (2000) Endoplasmic reticulum-derived compartments function in storage and as mediators of vacuolar remodelling via a new type of organelle, precursor protease vesicles. *Plant Physiol.* **123**, 1227–1233.
- Crofts, A.J., Leborgne-Castel, N., Hillmer, S., Robinson, D.G., Philipson, B., Carlsson, L.E., Ashford, D.A. and Denecke, J. (1999) Saturation of the endoplasmic reticulum retention machinery reveals anterograde bulk flow. *Plant Cell*, **11**, 2233–2247.
- Denecke, J., Botterman, J. and Deblaere, R. (1990) Protein secretion in plant cells can occur via a default pathway. *Plant Cell*, **2**, 51–59.
- Denecke, J., De Rycke, R. and Botterman, J. (1992) Plant and mammalian sorting signals for protein retention in the endoplasmic reticulum contain a conserved epitope. *EMBO J.* **11**, 2345–2355.
- Dreier, L. and Rapoport, T.A. (2000) *In vitro* formation of the endoplasmic reticulum occurs independently of microtubules by a controlled fusion reaction. *J. Cell Biol.* **148**, 883–898.
- Galway, M.E., Heckman, J.W. and Schiefelbein, J.W. (1997) Growth and ultrastructure of *Arabidopsis* root hairs: the *rhd3* mutation alters vacuole enlargement and tip growth. *Planta*, **201**, 209–218.
- Geelen, D., Leyman, B., Batoko, H., Di Sansebastiano, G.P., Moore, I. and Blatt, M.R. (2002) The abscisic acid-related SNARE homolog NtSyr1 contributes to secretion and growth: evidence from competition with its cytosolic domain. *Plant Cell*, **14**, 387–406.
- Geldner, N., Friml, J., Stierhof, Y.D., Jurgens, G. and Palme, K. (2001) Auxin transport inhibitors block PIN1 cycling and vesicle trafficking. *Nature*, **413**, 425–428.
- Geldner, N., Anders, N., Wolters, H., Keicher, J., Kornberger, W., Muller, P., Delbarre, A., Ueda, T., Nakano, A. and Jurgens, G. (2003) The *Arabidopsis* GNOM ARF-GEF mediates endosomal recycling, auxin transport, and auxin-dependent plant growth. *Cell*, **112**, 219–230.
- Gomord, V., Denmat, L.A., Fitchette-Laine, A.C., Satiat-Jeuemaitre, B., Hawes, C. and Faye, L. (1997) The C-terminal HDEL sequence is sufficient for retention of secretory proteins in the endoplasmic reticulum (ER) but promotes vacuolar targeting of proteins that escape the ER. *Plant J.* **11**, 313–325.
- Grebe, M., Xu, J., Mobius, W., Ueda, T., Nakano, A., Geuze, H.J., Rook, M.B. and Scheres, B. (2003) *Arabidopsis* sterol endocytosis involves actin-mediated trafficking via ARA6-positive early endosomes. *Curr. Biol.* **13**, 1378–1387.
- Haseloff, J., Siemerling, K.R., Prasher, D.C. and Hodge, S. (1997) Removal of a cryptic intron and subcellular localization of green fluorescent protein are required to mark transgenic *Arabidopsis* plants brightly. *Proc. Natl. Acad. Sci. USA*, **94**, 2122–2127.
- Hawes, C., Saint-Jore, C., Martin, B. and Zheng, H. (2001) ER confirmed as the location of mystery organelles in *Arabidopsis* plants expressing GFP! *Trends Plant Sci.* **6**, 245–246.
- Herman, E.M., Tague, B.W., Hoffman, L.M., Kjemtrup, S.E. and Chrispeels, M.J. (1990) Retention of phytohaemagglutinin with carboxyterminal tetrapeptide KDEL in the nuclear envelope and the endoplasmic reticulum. *Planta*, **182**, 305–312.
- Hu, Y., Zhong, R., Morrison, W.H. 3rd and Ye, Z.H. (2003) The *Arabidopsis* *RHD3* gene is required for cell wall biosynthesis and actin organization. *Planta*, **217**, 912–921.
- Jefferson, R.A., Kavanagh, T.A. and Bevan, M.W. (1987) GUS fusions: beta-glucuronidase as a sensitive and versatile gene fusion marker in higher plants. *EMBO J.* **6**, 3901–3907.
- Jones, A.M. and Herman, E.M. (1993) KDEL-containing auxin-binding protein is secreted to the plasma membrane and cell wall. *Plant Physiol.* **101**, 595–606.
- Jurgens, G. and Geldner, N. (2002) Protein secretion in plants: from the *trans*-Golgi network to the outer space. *Traffic*, **3**, 605–613.
- Kim, D.H., Eu, Y.J., Yoo, C.M., Kim, Y.W., Pih, K.T., Jin, J.B., Kim, S.J., Stenmark, H. and Hwang, I. (2001) Trafficking of phosphatidylinositol 3-phosphate from the *trans*-Golgi network to the lumen of the central vacuole in plant cells. *Plant Cell*, **13**, 287–301.
- Kosegarten, H., Grolig, F., Esch, A., Glusenkamp, K.H. and Mengel, K. (1999) Effects of  $\text{NH}_4^+$ ,  $\text{NO}_3^-$  and  $\text{HCO}_3^-$  on apoplast pH in the outer cortex of root zones of maize, as measured by the fluorescence ratio of fluorescein boronic acid. *Planta*, **209**, 444–452.
- Kunze, I.I., Hensel, G., Adler, K., Bernard, J., Neubohn, B., Nilsson, C., Stoltenburg, R., Kohlwein, S.D. and Kunze, G. (1999) The green fluorescent protein targets secretory proteins to the yeast vacuole. *Biochim. Biophys. Acta*, **1410**, 287–298.
- Li, X.Q., Zhang, G.H., Ngo, N., Zhao, X.N., Kain, S.R. and Huang, C.C. (1997) Deletions of the *Aequorea victoria* green fluorescent protein define the minimal domain required for fluorescence. *J. Biol. Chem.* **272**, 28545–28549.
- Liebe, S. and Quader, H. (1994) Myosin in onion (*Allium cepa*) bulb scale epidermal cells: involvement in dynamics of organelles and endoplasmic reticulum. *Physiol. Plant.* **90**, 114–124.
- Liu, S., Bugos, R.C., Dharmasiri, N. and Su, W.W. (2001) Green fluorescence protein as a secretory reporter and a tool for process optimization in transgenic plant cell cultures. *J. Biotechnol.* **87**, 1–16.

- Lukowitz, W., Mayer, U. and Jürgens, G. (1996) Cytokinesis in the *Arabidopsis* embryo involved the syntaxin-related KNOLLE gene product. *Cell*, **84**, 61–71.
- Matsushima, R., Kondo, M., Nishimura, M. and Hara-Nishimura, I. (2003) A novel ER-derived compartment, the ER body, selectively accumulates a beta-glucosidase with an ER-retention signal in *Arabidopsis*. *Plant J.* **33**, 493–502.
- Mellman, I. and Warren, G. (2000) The road taken: past and future foundations of membrane traffic. *Cell*, **100**, 99–112.
- Monroe, J.D., Gough, C.M., Chandler, L.E., Loch, C.M., Ferrante, J.E. and Wright, P.W. (1999) Structure, properties, and tissue localization of apoplastic  $\alpha$ -glucosidase in crucifers. *Plant Physiol.* **119**, 385–397.
- Nebenführ, A., Gallagher, L., Dunahay, T.G., Frohlick, J.A., Masurkiewicz, A.M., Meehl, J.B. and Staehelin, L.A. (1999) Stop-and-go movements of plant Golgi stacks are mediated by the actomyosin system. *Plant Physiol.* **121**, 1127–1141.
- Ortiz, D., Medkova, M., Walch-Solimena, C. and Novick, P. (2002) Ypt32 recruits the Sec4p guanine nucleotide exchange factor, Sec2p, to secretory vesicles: evidence for a Rab cascade in yeast. *J. Cell Biol.* **157**, 1005–1015.
- Parker, J.S., Cavell, A.C., Dolan, L., Roberts, K. and Grierson, C.S. (2000) Genetic interactions during root hair morphogenesis in *Arabidopsis*. *Plant Cell*, **12**, 1961–1974.
- Phillips, D.G., Preshaw, C. and Steer, M.W. (1988) Dictyosome vesicle production and plasma membrane turnover in auxin-stimulated outer epidermal cells of coleoptile segments from *Avena sativa* (L.). *Protoplasma*, **145**, 59–65.
- Pimpl, P., Hanton, S.L., Taylor, J.P., Pinto-DaSilva, L.L. and Denecke, J. (2003) The GTPase ARF1p controls the sequence-specific vacuolar sorting route to the lytic vacuole. *Plant Cell*, **15**, 1242–1256.
- Rojo, E., Gillmor, C.S., Kovaleva, V., Somerville, C.R. and Raikhel, N.V. (2001) *VACUOLELESS1* is an essential gene required for vacuole formation and morphogenesis in *Arabidopsis*. *Dev. Cell*, **1**, 303–310.
- Rutherford, S. and Moore, I. (2002) The *Arabidopsis* Rab GTPase family: another enigma variation. *Curr. Opin. Plant Biol.* **5**, 518–528.
- Saint-Jore, C.M., Evins, J., Batoko, H., Brandizzi, F., Moore, I. and Hawes, C. (2002) Redistribution of membrane proteins between the Golgi apparatus and endoplasmic reticulum in plants is reversible and not dependent on cytoskeletal networks. *Plant J.* **29**, 661–678.
- Sanderfoot, A.A., Assaad, F.F. and Raikhel, N.V. (2000) The *Arabidopsis* genome. An abundance of soluble *N*-ethylmaleimide-sensitive factor adaptor protein receptors. *Plant Physiol.* **124**, 1558–1569.
- Sansebastiano, G.P.D., Paris, N., Marc-Martin, S. and Neuhaus, J.M. (1998) Specific accumulation of GFP in a non-acidic vacuolar compartment via a C-terminal propeptide-mediated sorting pathway. *Plant J.* **15**, 449–458.
- Schiefelbein, J.W. and Somerville, C. (1990) Genetic control of root hair development in *Arabidopsis thaliana*. *Plant Cell*, **2**, 235–243.
- Shannon, T.M., Picton, J.M. and Steer, M.W. (1984) The inhibition of dictyosome vesicle formation in higher plant cells by cytochalasin D. *Eur. J. Cell Biol.* **33**, 144–147.
- Shevell, D.E., Leu, W.M., Gillmor, C.S., Xia, G., Feldmann, K.A. and Chua, N.H. (1994) *EMB30* is essential for normal cell division, cell expansion, and cell adhesion in *Arabidopsis* and encodes a protein that has similarity to Sec7p. *Cell*, **77**, 1051–1062.
- Sohn, E.J., Kim, E.S., Zhao, M. et al. (2003) Rha1, an *Arabidopsis* Rab5 homolog, plays a critical role in the vacuolar trafficking of soluble cargo proteins. *Plant Cell*, **15**, 1057–1070.
- Steinmann, T., Geldner, N., Grebe, M., Mangold, S., Jackson, C.L., Paris, S., Galweiler, L., Palme, K. and Jürgens, G. (1999) Coordinated polar localization of auxin efflux carrier PIN1 by GNOM ARF GEF. *Science*, **286**, 316–318.
- Takeuchi, M., Ueda, T., Sato, K., Abe, H., Nagata, T. and Nakano, A. (2000) A dominant negative mutant of Sar1p GTPase inhibits protein transport from the endoplasmic reticulum to the Golgi apparatus in tobacco and *Arabidopsis* cultured cells. *Plant J.* **23**, 517–525.
- Takeuchi, M., Ueda, T., Yahara, N. and Nakano, A. (2002) Arf1p GTPase plays roles in the protein traffic between the endoplasmic reticulum and the Golgi apparatus in tobacco and *Arabidopsis* cultured cells. *Plant J.* **31**, 499–515.
- Tamura, K., Shimada, T., Ono, E., Tanaka, Y., Nagatani, A., Higashi, S.I., Watanabe, M., Nishimura, M. and Hara-Nishimura, I. (2003) Why green fluorescent fusion proteins have not been observed in the vacuoles of higher plants. *Plant J.* **35**, 545–555.
- Toyooka, K., Okamoto, T. and Minamikawa, T. (2000) Mass transport of proform of a KDEL-tailed cysteine proteinase (SH-EP) to protein storage vacuoles by endoplasmic reticulum-derived vesicle is involved in protein mobilization in germinating seeds. *J. Cell Biol.* **148**, 453–463.
- Tsien, R.Y. (1998) The green fluorescent protein. *Annu. Rev. Biochem.* **67**, 509–544.
- Wandelt, C.I., Khan, M.R.I., Craig, S., Schroeder, H.E., Spencer, D. and Higgins, T.J.V. (1992) Vicilin with carboxyl-terminal KDEL is retained in the endoplasmic reticulum and accumulates to high levels in the leaves of transgenic plants. *Plant J.* **2**, 181–192.
- Wang, H., Lockwood, S.K., Hoeltzel, M.F. and Schiefelbein, J.W. (1997) The *ROOT HAIR DEFECTIVE 3* gene encodes an evolutionarily conserved protein with GTP-binding motifs and is required for regulated cell enlargement in *Arabidopsis*. *Gene Dev.* **11**, 799–811.
- Wang, H., Lee, M.M. and Schiefelbein, J.W. (2002) Regulation of the cell expansion gene *RHD3* during *Arabidopsis* development. *Plant Physiol.* **129**, 638–649.
- Yang, X., Matern, H.T. and Gallwitz, D. (1998) Specific binding to a novel and essential Golgi membrane protein (Yip1p) functionally links the transport GTPases Ypt1p and Ypt31p. *EMBO J.* **17**, 4954–4966.